An implicit high order cell-centered finite volume scheme for the solution of three-dimensional Navier–Stokes equations on unstructured grids

D. Vigneron[a,b,*], J.-M. Vaassen[a], J.-A. Essers[a]

[a] *Aerodynamics Group*

[b] *Turbomachinery Group Département AéroSpatial Mécanique et Matériaux (ASMA), Université de Liège, Institut de Mécanique et Génie Civil (Bât. B52/3), 1, Chemin des Chevreuils, B-4000 Liège, Belgium*

Abstract

This paper presents a finite volume solver for the computation of three-dimensional viscous flows. A cell-centered approach is used and a quadratic reconstruction of the unknowns is performed to compute the advective fluxes on the cell faces. The gradients of the variables, necessary for the viscous fluxes, are constructed using Coirier's diamond path. A extended version of this method is proposed in this paper to ensure the consistency of the method whatever the distortion of the grid. A fully implicit time integration procedure is employed with preconditioned matrix-free GMRES solver.

Keywords: Various flow regimes; Viscous flows; Finite volume solver; Quadratic reconstruction; Consistent viscous scheme; Newton–Krylov; Unstructured meshes

1. Introduction

In a finite volume method, the Navier–Stokes equations are integrated over mesh control volumes. This leads to Eq. (1) in which advective fluxes $\boldsymbol{F}_a$ and diffusive fluxes $\boldsymbol{F}_d$ are integrated over the surfaces delimiting the cells:

$$\frac{d\boldsymbol{s}}{dt}+\frac{1}{V}\int_S \boldsymbol{F}_a(\boldsymbol{w})\cdot\boldsymbol{n}\,dS=\frac{1}{V}\int_S \boldsymbol{F}_d(\boldsymbol{w},\nabla\boldsymbol{w})\cdot\boldsymbol{n}\,dS \qquad (1)$$

where $\boldsymbol{s}$ and $\boldsymbol{w}$ respectively denote the vectors for the conservative and primitive variables

$$\boldsymbol{s}=(\rho,\ \rho u_x,\ \rho u_y,\ \rho u_z,\ \rho E)^T \qquad \boldsymbol{w}=(\rho,\ u_x,\ u_y,\ u_z,\ T)^T \qquad (2)$$

with collecting velocity $\boldsymbol{u}$, fluid density ρ, pressure p, temperature T, and total energy E; $\boldsymbol{n}$ is the surface normal vector. This formulation ensures the conservativity of mass, momentum and total enthalpy through the computational domain as well as the Rankine-Hugoniot relations through discontinuities.

The solver is designed for three-dimensional unstructured meshes whose volume faces may be triangles or (possibly non-planar) quadrilaterals. It is based on a cell-centered approach so that the mean value of $\boldsymbol{s}$ over a cell is assumed to be equal to the value at the cell gravity center, leading to a second-order truncation error [1] for the advective derivatives. Consequently, neither the variables in $\boldsymbol{w}$ nor their gradients are available on the faces. A reconstruction procedure, described in section 2, is used for the advective terms evaluation. The gradient computation procedure is based on an extended version of Coirier's diamond path [2], presented in section 3, which provides a consistent discretization of the diffusive terms regardless of the irregularity of the mesh, and exhibits good positivity properties.

A fully implicit time integration procedure is employed. The Newton method is used to linearize the equations resulting from the implicit discretization, and the linear systems are solved by a preconditioned matrix-free GMRES solver [3].

Finally, two test cases are presented to illustrate the good accuracy properties of the solver.

* Corresponding author. Tel.: +32 436 69439; Fax: +32 436 69136; E-mail: @Didier.Vigneron@ulg.ac.be

Computational Fluid and Solid Mechanics 2005
K.J. Bathe (Editor)

2. Advective terms discretization

The advective fluxes discretization consists in integrating, by use of a Gauss quadrature formula, a numerical flux $\tilde{\boldsymbol{F}}(\tilde{\boldsymbol{w}}_R, \tilde{\boldsymbol{w}}_L)$ over a face separating the nodes L and R respectively. The computation of $\tilde{\boldsymbol{F}}$ is performed by Roe's flux difference splitting [4], Van Leer's flux vector splitting or by an advective upstream splitting method (AUSM) [5]. The reconstructed values $\tilde{w}_R$ and $\tilde{w}_L$ are evaluated by a Taylor expansion:

$$\tilde{w}_{R,L} = w_{R,L} + (\boldsymbol{x}_G - \boldsymbol{x}_{R,L})^T \nabla w_{R,L} + \frac{1}{2}(\boldsymbol{x}_G - \boldsymbol{x}_{R,L}) H_{R,L} (\boldsymbol{x}_G - \boldsymbol{x}_{R,L}) + \mathcal{O}(h^3) \tag{3}$$

where $\boldsymbol{x}_G$ denotes the positions of the Gauss points, and the hessian matrix $\boldsymbol{H}$ contains the second derivatives of $\tilde{w}_{R,L}$. A constant reconstruction scheme (first-order) only uses the left and right neighbours' values but is proven to be inconsistent on irregular meshes. A linear reconstruction is necessary to ensure consistency. It requires the computation of a first-order approximation of the gradient, and one (four) Gauss points for a triangular (quadrangular) face. A third-order method, which leads to second-order truncation errors, is obtained by using a quadratic reconstruction and three (four) Gauss points for a triangular (quadrangular) face. Such a scheme requires a second-order approximation of the gradient and a first-order one for the hessian matrix.

The necessary derivatives are constructed as a linear combination of node values over a selected stencil, the weights being generated by a least square method [1].

3. Diffusive terms discretization

The diffusive fluxes of a newtonian fluid can be written

$$\boldsymbol{F}_d = \begin{pmatrix} \boldsymbol{0}^T \\ \mu \left[\nabla \boldsymbol{u} + (\nabla \boldsymbol{u})^T\right] - \frac{2}{3}\mu\,(\nabla \cdot \boldsymbol{u})\,\boldsymbol{I} \\ \mu\, \boldsymbol{u}^T \left[\nabla \boldsymbol{u} + (\nabla \boldsymbol{u})^T\right] - \frac{2}{3}\mu\,(\nabla \cdot \boldsymbol{u})\,\boldsymbol{u}^T + k \nabla T \end{pmatrix} \tag{4}$$

Their integration is performed by a Gauss quadrature formula, requiring the gradients to be computed at each face Gauss point. To obtain a consistent discretization regardless of the irregularity of the grid, a second-order approximation of the gradients is required.

A compact scheme based on Coirier's diamond path [2] is first generalized in three dimensions. This method exhibits very good positivity properties, which avoids the appearance of oscillations in the solution. The diamond path is built by connecting each vertex of a face to the left (L) and right (R) neighbour nodes, forming a polyhedron Ω (of surface Σ) on which a Green-Gauss formula is applied to compute the gradient at the face center P:

$$\nabla w_P = \frac{1}{\Omega} \int_\Sigma w\, \boldsymbol{n}\, d\Sigma + \mathcal{O}(h) \tag{5}$$

The integration over the triangles of Σ is easily performed, so that $\nabla \omega_p$ appears as a linear combination of values of $\boldsymbol{w}$ at L, R and at the face vertices. The latter are reconstructed with a second-order accuracy from the nodes surrounding the vertex. This discretization only leads to a first-order approximation of the gradient on the faces because P does not necessarily coincide with the gravity center of Ω. The global scheme is thus inconsistent on irregular grids.

An original modification is now proposed to restore unconditional consistency (i.e. to obtain at least a first-order truncation error for the diffusive derivatives) while keeping the good positivity properties of the diamond scheme. In the latter, the gradient is finally computed as a linear combination of the unknowns at a set of nodes surrounding the face. The weights, stored in $\bar{\beta}$, are now modified by a correction $\Delta\beta$ in order to reach the necessary approximation. For example, the x-derivative must verify the following constraints of accuracy:

$$\boldsymbol{A}^{\boldsymbol{T}}(\overline{\beta} + \Delta\beta) = \boldsymbol{d} \qquad \boldsymbol{A} = \begin{pmatrix} \boldsymbol{v}_1^T \\ \boldsymbol{v}_2^T \\ \vdots \\ \boldsymbol{v}_N^T \end{pmatrix}$$

$$\boldsymbol{v}_i = \begin{pmatrix} 1 \\ x_i - x_p \\ y_i - y_p \\ z_i - z_p \\ \frac{1}{2}(x_i - x_p)^2 \\ \frac{1}{2}(y_i - y_p)^2 \\ \frac{1}{2}(z_i - z_p)^2 \\ (x_i - x_p)\,(y_i - y_p) \\ (y_i - y_p)\,(z_i - z_p) \\ (z_i - z_p)\,(x_i - x_p) \end{pmatrix} \qquad \boldsymbol{d} = \begin{pmatrix} 0 \\ 1 \\ 0 \\ 0 \\ 0 \\ 0 \\ 0 \\ 0 \\ 0 \\ 0 \end{pmatrix} \tag{6}$$

As the number of nodes in the stencil is greater than the number of constraints, we can impose that the weights must be as close as possible to the values of the diamond scheme, to keep the good positivity properties of this method. This leads to minimizing

$$z = \frac{1}{2} \sum_{i=1}^{N} \Delta\beta_i^2 \tag{7}$$

This optimization problem is then solved by the Lagrange's multipliers technique, leading to the following corrections:

$$\Delta\beta^T = (\boldsymbol{d} - \boldsymbol{A}^T\overline{\beta})^T (\boldsymbol{A}^T\boldsymbol{A})^{-1}\boldsymbol{A}^T \tag{8}$$

This computation has been performed for the face center P, which is the Gauss point on a triangular face. For a quadrangular one, the correction should actually be performed for the four Gauss points G. Rather than repeating the procedure, it is more easy to use

$$\nabla w_G = \nabla w_P + \boldsymbol{H}\,(\boldsymbol{x}_G - \boldsymbol{x}_P) + \mathcal{O}(h^2) \tag{9}$$

where the hessian matrix $\boldsymbol{H}$ is evaluated in the same way as for the advective terms.

4. Boundary conditions treatment

The boundary conditions at the inflow and outflow boundaries are imposed in the fluxes, i.e. in a weak way. At solid walls, no-slip conditions are imposed in a strong way, the boundary nodes being moved to the boundary:

$$u_x = u_y = u_z = 0 \qquad T = T_{wall} \qquad or \qquad \frac{\partial T}{\partial n} = 0 \tag{10}$$

5. Newton-GMRES scheme

A fully implicit scheme has been developed to overcome the difficulties arising from the severe non-linearities of our problems.

An iterative Newton method is aimed at the resolution of the non-linear systems

$$\frac{d\boldsymbol{s}}{dt} + F(\boldsymbol{s}) = 0 \tag{11}$$

This method performs a linearization of the equations at each time step, leading to the following linear system to be solved:

$$\left[\frac{1}{\Delta t}\boldsymbol{I} + J\left(\boldsymbol{s}^{(n)}\right)\right]\delta\boldsymbol{s}^{(n)} = -F\left(\boldsymbol{s}^{(n)}\right) \tag{12}$$

where J denotes the Jacobian matrix of F, and Δt is the time step. In order to increase the convergence speed, this time step is computed according to the switched evolution relaxation (SER) method [6], which increases it inversely to the residual norm reduction.

The generalized minimal residual (GMRES) algorithm [3], based on a Krylov subspace method, is used to iteratively solve the linear system (12). In this algorithm, the full Jacobian matrix J is not required explicitly (matrix-free algorithm) but rather in the form of matrix-vector products, which can be computed by the finite difference formula

$$J\left(\boldsymbol{s}^{(n)}\right)v \approx \frac{F\left(\boldsymbol{s}^{(n)} + \epsilon v\right) - F\left(\boldsymbol{s}^{(n)}\right)}{\epsilon} \tag{13}$$

This implementation avoids the costing storage and computation of the Jacobian matrix. A preconditioner reducing the conditioning number of the system is required, however, to ensure good convergence of the GMRES solver. Right preconditioning based on a block incomplete factorization (BILU(k)) of an approximate Jacobian is employed [7]. This Jacobian matrix is computed with a constant reconstruction for the advective terms and a classical diamond path for the viscous ones.

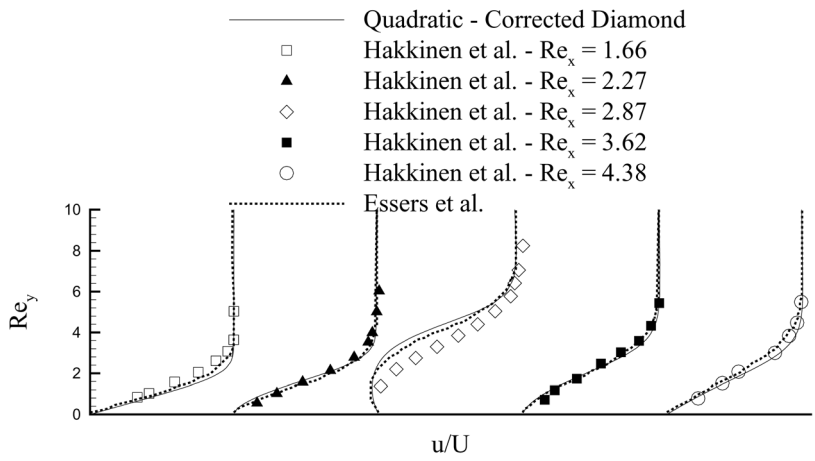

Fig. 1. Shock–boundary layer interaction on adiabatic flat plate. X-component velocity profile at shock impingement. Results obtained with a quadratic reconstruction for the advective terms and the corrected diamond scheme for diffusive terms. The results are compared with the computation on a bi-dimensional quadrangular mesh from Essers et al. [9].

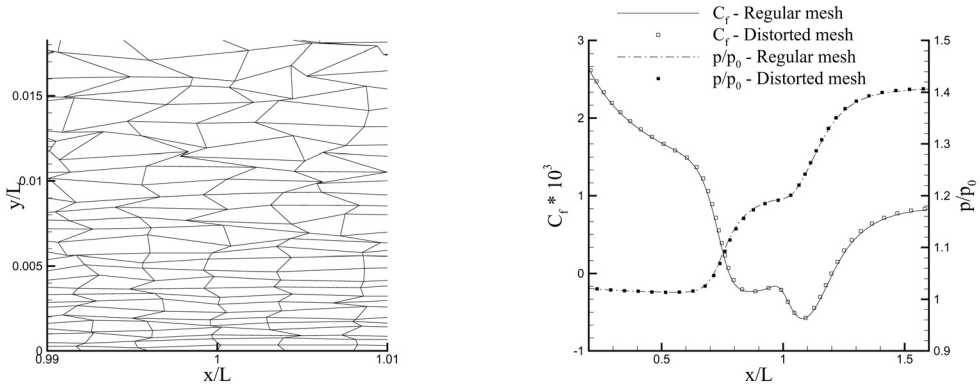

Fig. 2. Shock–boundary layer interaction on adiabatic flat plate. (a) Distorted mesh at the shock impingement. (b) Skin friction and pressure distribution on the flat plate. Computation made with a quadratic reconstruction for the advective terms and the corrected diamond scheme for the diffusive terms on regular and distorted grids.

6. Results

The solver has been tested on two flow regimes: a shock–boundary layer interaction and a subsonic flow past a sphere. The perfect gas law is supposed and the viscosity is evaluated by Sutherland's law.

6.1. Shock–boundary layer interaction

The two-dimensional flow over an adiabatic flat plate is studied on an extruded three-dimensional mesh. The free stream Mach number and temperature are respectively equal to 2 and 156 K, and the Reynolds number is 2.96×10^5. The initial two-dimensional mesh is composed of 18,000 cells (quandrangles in the boundary layer and triangles everywhere else) and extruded six times. The first point near the plate is located at $y/L = 3 \times 10^{-4}$ where the characteristic length L is the distance between the plate leading edge and the shock impingement point. A mesh with severe distortion, presented in Fig. 2(a), is also created from the latter.

Fig. 1 shows the x-component velocity profiles in the recirculation zone at the shock impingement, computed with the corrected diamond scheme and a quadratic reconstruction for the advective terms on the distorted grid. The comparison with the experimental results of Hakkinen et al. [8] and previous numerical computations of Essers et al. [9] depicts good agreement. The remarkably weak sensitivity of the solver to severe mesh distortions is demonstrated in Fig. 2(b) where skin friction and pressure distribution are presented.

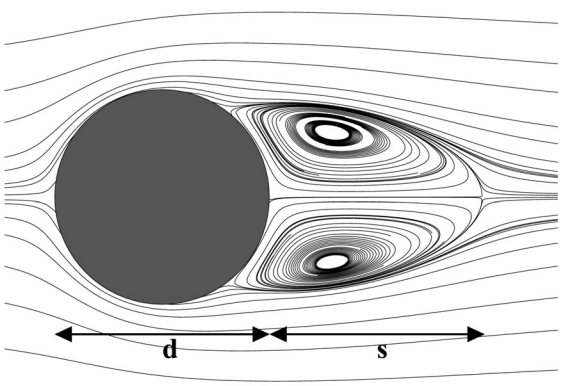

Fig. 3. Streamlines around the sphere for $Re = 118$. d = diameter. s = length of closed streamlines behind the sphere.

6.2. Flow past a sphere

A subsonic flow past an isothermal sphere is studied. The free stream Mach number and temperature are respectively equal to 0.2 and 300 K, and the sphere temperature is also 300 K. The mesh is composed of 270,000 tetrahedra. The flow has been computed for Reynolds numbers equal to 118, 73.6 and 37.7. The streamlines composed of a closed ring vortex behind the sphere for $Re = 118$ are shown on Fig. 3. The length of the recirculation zones are compared with the experimental results of Taneda [10] on Fig. 4. A linear reconstruction must be used for the advective terms to avoid too large numerical dissipation. Surprisingly, the corrected diamond only introduces a small improvement of the solution, even on a distorted mesh. The diamond scheme, even if theoretically inconsistent, seems to provide sufficiently accurate solutions.

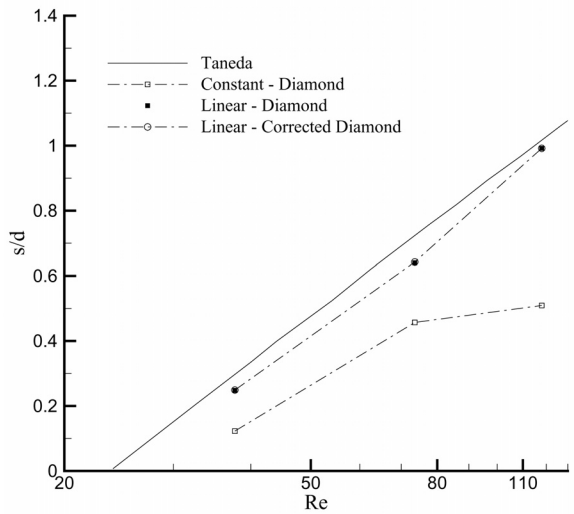

Fig. 4. Length of closed streamlines region behind the sphere for different Reynolds numbers. Comparison with experimental results from Taneda [10].

7. Conclusions

A finite volume solver has been developed for the computation of three-dimensional viscous flows. It uses high-order methods such as quadratic reconstruction for the computation of advective terms. A consistent version of Coirier's diamond path has been studied. Numerical results have proven the very good accuracy of the solutions, even on highly distorted grids. The corrected diamond scheme appeared to improve the quality of the solution but the classical scheme is quite accurate, even if it is inconsistent.

References

[1] Lepot I, Meers F, Essers J-A. Multilevel parallel high order schemes for inviscid flow computations on 3D unstructured meshes. In: Proc of the ECCOMAS Computational Fluid Dynamics Conference, K Morgan, NP Weatherill, editors, Swansea, Wales, 4–7 September 2001.

[2] Coirier WJ. An adaptively-refined, cartesian, cell-based scheme for the Euler and Navier-Stokes equations. PhD thesis, University of Michigan, June 1994.

[3] Saad Y, Schultz MH. GMRES: a Generalized Minimum Residual algorithm for solving non-symmetric linear systems. SIAM J Sci Stat Comput 1986;7(3):856–869.

[4] Roe PL. Approximate Riemann solver, parameter vectors and difference scheme. J Comput Phys 1981;43:357–372.

[5] Liou MS, Steffen JC. A new flux splitting scheme. J Comput Phys 1993;107:23–39.

[6] Mulder WA, van Leer B. Experiments with implicit upwind methods for the Euler equations. J Comput Phys 1985;59:232–246.

[7] Geuzaine P, Essers J-A, Lepot I, Meers F. Multilevel Newton-Krylov algorithms for computing compressible flows on unstructured meshes. AIAA Paper 99–3341, 1999.

[8] Hakkinen RJ, Greber I, Trilling L, Abarbanel SS. The interaction of an oblique shock wave with a laminar boundary layer. NASA Memo 2–18–59W, 1959.

[9] Essers J-A, Delanaye M, Rogiest P. An upwind-biased finite-volume technique solving compressible Navier-Stokes equations on irregular meshes. Applications to supersonic blunt-body flows and shock-boundary layer interactions. In: Proc of 11th AIAA Computational Fluid Dynamics Conference, June 1993, AIAA–93–3377.

[10] Batchelor GK. An Introduction to Fluid Dynamics. Cambridge: Cambridge University Press, 1967.